ORIGINAL RESEARCH ARTICLE

Interdiffusion Coefficients and Strengthening Effects of Nb, Ta, and Zr in the α2-Ti3Al Phase

L. Haußmann[1] · J. Bresler[1] · S. Neumeier[1] · F. Pyczak[2] · M. Göken[1]

Abstract The creep properties of fully lamellar γ/α2 titanium aluminides can be significantly improved by alloying with Nb, Ta or Zr. While the influence of these alloying elements on the γ-phase has already been examined, their diffusivity and strengthening properties in the α2-phase are still lacking. In order to study the effect of Nb, Ta and Zr in α2-Ti3Al, the alloys Ti-33Al, Ti-33Al-5Nb, Ti-33Al-5Ta and Ti-33Al-5Zr were investigated using a diffusion couple approach and strain rate jump tests. The results show that Zr diffuses the fastest, followed by Nb and Ta. Furthermore, these alloying elements also increase the strength compared to a binary Ti-33Al alloy, from which Zr leads to the highest strength increase followed by Ta and Nb. The lower diffusivity of Ta becomes increasingly important at higher temperatures and lower strain rates resulting in a higher strengthening potential than Nb and Zr under such conditions.

Keywords α2-phase · alloying elements · diffusion · solid solution · strain rate jump test · titanium aluminides · Ti3Al

✉ L. Haußmann
lukas.haussmann@fau.de

✉ S. Neumeier
steffen.neumeier@fau.de

1   Materials Science and Engineering, Institute I, Friedrich-Alexander-Universität Erlangen-Nürnberg (FAU), Martensstr. 5, 91058 Erlangen, Germany

2   Institute of Materials Physics, Helmholtz-Zentrum Hereon, Max-Planck-Str. 1, 21502 Geesthacht, Germany

1 Introduction

With a steady increase in global energy requirements, thermodynamically more efficient and environmentally friendly energy conversion systems are becoming increasingly important. New classes of materials are required to further increase efficiency, since the well-established Ni-base alloys have been developed almost to their limits over the last 50 years.[1,2] Titanium aluminides (TiAl) are an interesting alternative due to their good high-temperature strength, oxidation resistance and particularly low density.[3–7] The mechanical properties of these intermetallic alloys are strongly influenced by the microstructure. The fully or nearly lamellar microstructure with large colonies (50-100 μm) of alternating α2- and γ-lamellae exhibits relatively high fracture toughness and excellent creep strength. Consequently, such a microstructure is very important for technically relevant TiAl alloys.[1,4,8–11] The lamellar spacing in these alloys has a large influence on the mechanical properties. For example, the creep strength increases with decreasing lamellar spacing.[9,12] To improve the mechanical properties of lamellar microstructures even further, alloying elements can be added. Previous investigations showed that 5 at.% of Nb, Ta or Zr leads to an improved creep resistance,[12] which was attributed to the low diffusivity and high solid solution hardening coefficients of these alloying elements, which has already been shown for the γ-phase.[13]

In general, numerous studies on the influence of alloying elements on the mechanical properties have been carried out on the less hard and more ductile γ-phase,[1,12–17] since the γ-phase carries the majority of the deformation, especially at low temperatures.[1,18–20] However, intensive studies of alloying of the α2-phase are missing, especially for alloying elements other than Nb.[21–23] Furthermore, the

partitioning behavior between the γ- and α$_2$-phase in fully lamellar TiAl alloys can vary largely for the alloying elements. Zr tends to partition to the γ-phase, while Ta shows a slightly preferential partitioning to the α$_2$-phase.[17,24–28] For Nb, an approximately equal distribution between the γ- and α$_2$-phase[24,27,28] but also a slight tendency to partition to the γ-phase[17,25,26,29] is reported in literature. The α$_2$-phase becomes increasingly important for lamellar TiAl alloys at higher temperatures, as transmission electron microscopy (TEM) investigations show a steadily increasing plastic deformation of the α$_2$-phase with increasing temperature, where the diffusivity of alloying elements in the α$_2$-phase becomes more pronounced.[21,22,30] In this study, diffusion couples were used to determine the interdiffusion coefficients of the alloying elements Nb, Ta and Zr in the α$_2$-phase. In addition, strain rate jump (SRJ) compression tests at temperatures up to 900 °C were performed on single α$_2$-phase Ti-33Al and Ti-33Al-5X (X = Nb, Ta, Zr) alloys to study the temperature dependent strengthening potential of the alloying elements Nb, Ta and Zr.

2 Experimental Methods

The nominal composition of the investigated binary Ti-33Al alloy and the ternary Ti-33Al-5X (X = Nb, Ta, Zr) alloys is given in Table 1. The aluminum content of 33 at.% was chosen instead of the stoichiometric composition of Ti-25Al of α$_2$-Ti$_3$Al as the Ti-Al phase diagram[31] and atom probe measurements[17] revealed an aluminum content of 32 at.% to 35 at.% Al in the α$_2$-phase of the technically relevant fully lamellar TiAl alloys. Furthermore, CALPHAD calculations using the software Thermo-Calc with the database TCTi2 and the Ti-Al phase diagram[31] show a maximum of the order-disorder transformation temperature for the binary α$_2$-phase between 32 at.% and 34 at.% Al. This allows the interdiffusion heat treatment to be carried out at higher temperatures without an order-disorder transformation, resulting in a sufficient width of the interdiffusion zone in a shorter time.

The alloys were produced by vacuum arc melting from technically pure metals at the *Helmholtz-Zentrum Hereon* (*Geesthacht/Germany*) to buttons with a diameter of about 30 mm. All four alloys were heat treated at 1150 °C for 8 h to homogenize and adjust the microstructure. For the microstructural characterization, samples of the alloys were mechanically ground and then electropolished (*A3 electrolyte, Struers GmbH, Ottensoos/Germany*) at 60 V and a temperature between − 10 and − 40 °C, cooled by liquid nitrogen. The microstructure was analyzed using a scanning electron microscope (SEM) (*Crossbeam 1540 EsB, Carl Zeiss AG, Oberkochen/Germany*) and the chemical analysis was done using energy dispersive x-ray spectroscopy (EDS) (*Inca Energy 350, Oxford Instruments, Abingdon/United Kingdome*).

Table 1 Nominal composition of Ti-33Al and the Ti-33Al-5X alloys in at.%

	Ti	Al	Nb	Ta	Zr
Ti-33Al	67	33			
Ti-33Al-5Nb	62	33	5		
Ti-33Al-5Ta	62	33		5	
Ti-33Al-5Zr	62	33			5

The microstructure analysis was conducted with 20 kV excitation voltage using the back-scattered electron (BSE) detector and a 120 μm aperture. The EDS measurements were performed at 20 kV, 8 mm working distance, a 30 μm aperture and 100 s measurement time. A standard calibration procedure using a Co reference was performed prior to the measurements.

Each diffusion couple consisted of two cuboids (∼6 × 6 × 3 mm) of Ti-33Al and Ti-33Al-5X (X = Nb, Ta, Zr), respectively. One side of these cuboids was ground and polished as described above, and both samples were placed with the polished surfaces together in a molybdenum holder and fixed with molybdenum screws and alumina shims. This method has already been used in (Ref 13). The diffusion couples were heat treated in a vacuum furnace at 1050 °C for 500 h, at 1100 °C for 400 h or at 1150 °C for 300 °h. The concentration profiles were investigated by EDS, fitted with a dose-response function using a Levenberg-Marquadt algorithm[32] and evaluated according to the Sauer-Freise method[33] to determine the interdiffusion coefficients. Due to limitations of this method, the beginning and the end of the concentration profiles were not considered for the determination of the interdiffusion coefficients and only the data between 1.5 at.% and 3.5 at.% of the respective alloying element X was used.

To investigate the temperature-dependent influence of the alloying elements Nb, Ta and Zr on the mechanical properties, strain rate jump tests were performed in compression mode in air on an Instron 4505 (*Instron, Norwood, MA/USA*) modernized by Hegewald & Peschke (*Hegewald & Peschke Meß und Prüftechnik GmbH, Nossen/Germany*) using cylindrical specimens at room
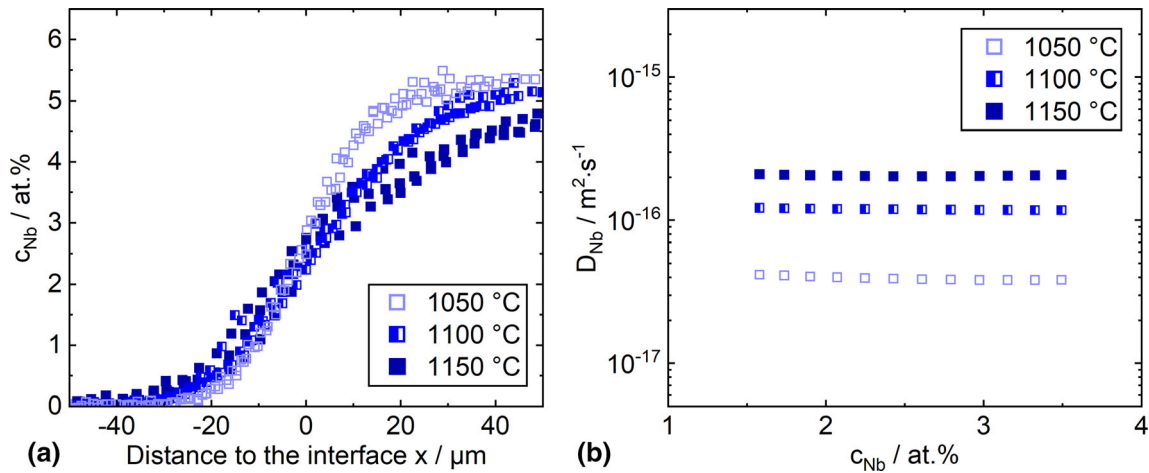
Fig. 1 (a) Concentration c_{Nb} of Nb across the interdiffusion zone after annealing at 1050, 1100 and 1150 °C. (b) Interdiffusion coefficient D_{Nb} as a function of the Nb concentration c_{Nb} at the three different annealing temperatures

temperature, 750 and 900 °C. The specimens were produced by spark erosion to a diameter of 4 mm. They were then ground to a parallel height of 6-7.5 mm. The strain rate was varied between 10^{-3}, 10^{-4} and 10^{-5} s^{-1} and the strain rate sensitivity was determined analogously to (Ref [13]) at the first and fourth strain rate jump according to (Ref [34], [35]).

3 Data Evaluation

Figure 1(a) shows exemplarily the measured concentration profiles of the Nb-containing diffusion couples (Ti-33Al/Ti-33Al-5Nb), aged at 1050, 1100 and 1150 °C, respectively. All three curves show the expected S-shape. The Nb concentration increases from 0 at.% on the binary side to about 5.0–5.5 at.% Nb on the ternary side. The different Nb concentrations on the Ti-33Al-5Nb side could be due to casting segregations, which are still present due to the low initial heat treatment temperature, or due to measurement-related errors of the EDS measurement. However, since the alloying element concentration does not change significantly at the different measurement locations, the effect on the interdiffusion coefficients is negligible. The resulting interdiffusion coefficients between 1.5 at.% and 3.5 at.% Nb are shown in Fig. 1(b).

Usually, the diffusion couple approach has the great advantage that the solid solution hardening coefficient can be determined on the same sample in addition to the interdiffusion coefficient by performing nanoindentations across the interdiffusion zone. However, the hardness of the single α_2-phase alloys determined by nanoindentations

at room temperature showed a strong dependence on the grain orientation and could not be used to determine solid solution hardening coefficients. A possible explanation for the strong orientation dependence of the hardness could be due to the significantly different activation energies of the three slip systems in Ti$_3$Al and the resulting limited ductility at room temperature.[1,22,36]

Since the analysis of the other diffusion couples showed similar concentration profiles, only the results of these investigations are presented and discussed in the following chapter. The data evaluation of the diffusion couples with the other two ternary alloys Ti-33Al-5Ta and Ti33Al-5Zr is shown in the Supplementary Information in the Figures S1 and S2.

4 Results and Discussion

4.1 Interdiffusion Coefficients

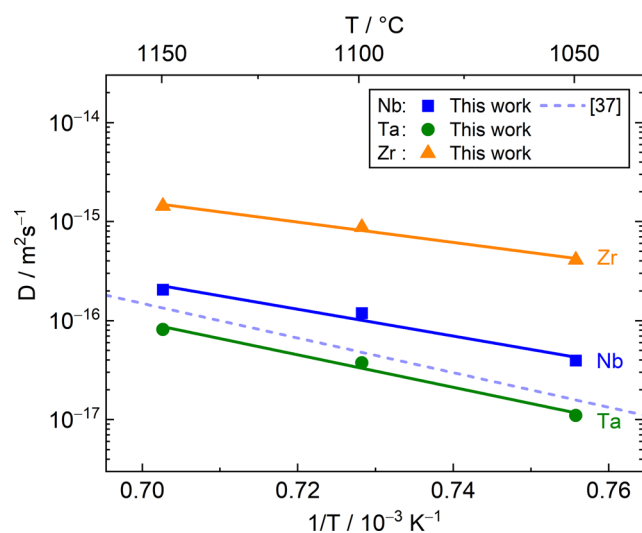The determined average interdiffusion coefficients of Nb, Ta and Zr in Ti-33Al are listed in Table 2.

The results are shown in an Arrhenius diagram in Fig. 2 together with literature data for the diffusion of Nb in α_2-Ti$_3$Al.[37]

The activation energy Q (kJ·mol^{-1}) and the frequency factor D_0 (m^2·s^{-1}) were calculated using equation 1, where R (J·mol^{-1}·K^{-1}) is the universal gas constant and T (K) is the temperature, see Table 3.

$$D = D_0 \cdot \exp\left(-\frac{Q}{R \cdot T}\right) \qquad \text{(Eq 1)}$$

Table 2 Average interdiffusion coefficient of Nb $\overline{D}_{Nb}$, Ta $\overline{D}_{Ta}$ and Zr $\overline{D}_{Zr}$ in α_2-Ti-33Al

Temperature	$\overline{D}_{Nb}$, m^2 s^{-1}	$\overline{D}_{Ta}$, m^2 s^{-1}	$\overline{D}_{Zr}$, m^2 s^{-1}
1050 °C	3.94×10^{-17}	1.10×10^{-17}	4.08×10^{-16}
1100 °C	1.19×10^{-16}	3.74×10^{-17}	8.73×10^{-16}
1150 °C	2.06×10^{-16}	8.15×10^{-17}	1.43×10^{-15}

Fig. 2 Arrhenius plot of the average interdiffusion coefficients D of Nb, Ta and Zr determined in this work together with literature data from Breuer et al.,[37] which were extrapolated to a temperature of 1150 °C

Table 3 Activation energy Q and frequency factor D_0 of the alloying elements Nb, Ta and Zr α_2-Ti-33Al

Element	Activation energy Q, kJ mol^{-1}	Frequency factor, m^2 s^{-1}
Nb	262	8.25×10^{-7}
Ta	317	3.32×10^{-5}
Zr	199	2.64×10^{-8}

Since the heat treatment temperature of 1150 °C is near the order-disorder transformation temperature of the binary α_2-phase, CALPHAD calculations were carried out for the binary and the three ternary alloys using the software Thermo-Calc with the database TCTi2. The order-disorder transformation temperatures could be determined as 1189 °C for Ti-33Al, 1283 °C for Ti-33Al-5Nb, 1132 °C for Ti-33Al-5Ta and 1157 °C for Ti-33Al-5Zr. While the order-disorder transformation temperatures of Ti-33Al and Ti-33Al-5Nb are well above the heat treatment temperature of 1150 °C, the order-disorder transformation temperature of Ti-33Al-Ta and Ti-33Al-5Zr is below and slightly above 1150 °C, respectively. Nevertheless, we could not observe an increasing interdiffusion coefficient with increasing Ta or Zr concentration and the activation energies for the diffusion of Ta and Zr agree quite well with that of Nb, while the diffusion coefficient in the disordered α-phase should be in the range of orders of magnitudes larger than in the ordered α_2-phase. We therefore assume a negligible influence of order-disorder transformation processes in our experiments.

The results in Table 2 and Fig. 2 show that Ta has the lowest diffusivity, followed by Nb and then Zr. The interdiffusion coefficients of all three alloying elements show an exponential behavior with increasing temperature. Nb, Ta and Zr are all occupying sites in the Ti sublattice,[38] which suggests very similar diffusion mechanisms. Compared to literature data for the diffusion of Nb in α_2-Ti$_3$-Al,[37] the measured interdiffusion coefficients are slightly larger. This difference could be due to the different methods used to determine the interdiffusion coefficients, since the results in (Ref 37) were obtained using the radiotracer method. For Ta and Zr no literature data are available so far. However, the trend in the diffusivity of the three elements is the same as observed in single γ-phase TiAl alloys[13] and is also found in other metallic materials such as Ni[39] or Co[40] solid solutions.

Similar to the recent results on the single γ-phase Ti-54Al alloys, the diffusion coefficients in this study also seem to correlate with the Goldschmidt radii,[41] where larger atoms diffuse faster. This behavior was already observed by Janotti et al.,[42] who studied the diffusion of different transition metal solutes in Ni using first-principle calculations. It was proposed that the larger transition metal atoms have a higher compressibility and form weaker bonds to the atoms of the host lattice, which leads to increased solute-vacancy exchanges and therefore a faster diffusion.[39,42] The compressibility of the solutes can also explain the lower diffusion coefficient of Ta compared to Nb, despite having a very similar Goldschmidt radius. Transition metals of the 5d-series exhibit a generally lower compressibility than those of the 4d-series. The findings by Janotti et al.[42] and Fu et al.[39] are also supported by experimentally determined diffusion coefficients for different solutes in Ni.[43–45]

4.2 Strain Rate Jump Tests

To evaluate the mechanical properties of the single phase Ti-33Al-5X alloys, strain rate jump tests were performed at room temperature, 750 and 900 °C in compression mode in air. It should be noted that the heat treatment at 1150 °C for
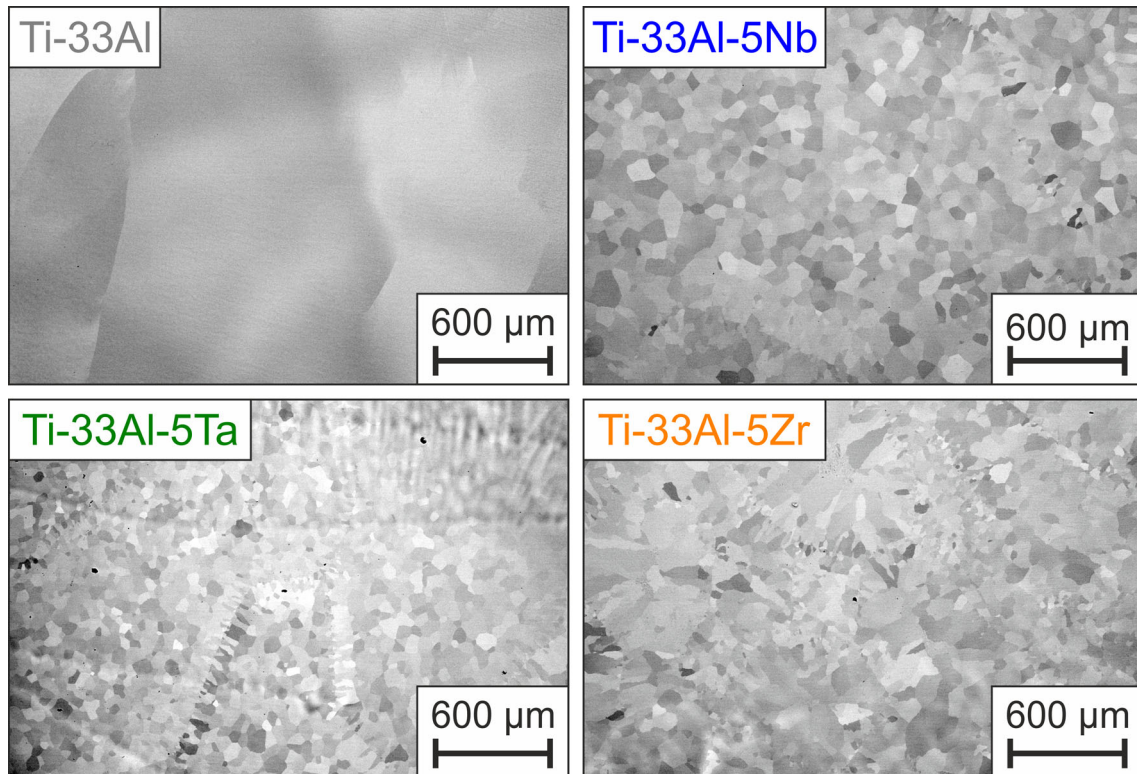
Fig. 3 SEM images in BSE mode of the microstructures of the binary Ti-33Al and the ternary Ti-33Al-5X alloys after a heat treatment at 1150 °C for 8 h

8 h resulted in a recrystallized microstructure of the ternary Ti-33Al-5Nb, Ti-33Al-5Ta and Ti-33Al-5Zr alloys with an average grain size of 65 μm, 45 μm and 50 μm, respectively, while the binary Ti-33Al alloy showed no signs of recrystallization resulting in a larger average grain size of 491 μm, as shown in Fig. 3.

To account for the different grain size , the Hall-Petch strengthening contribution σ_{HP} was estimated using equation 2 with the Hall-Petch constant k_{HP} and the grain size d.[7,46] Since no Hall-Petch constant was available for α_2-Ti_3Al, the value for hcp Ti of 12 MPa·mm$^{-0.5}$ [47] was used.

$$\Delta\sigma_{HP} = \frac{k_{HP}}{\sqrt{d}} \qquad \text{(Eq 2)}$$

The calculated Hall-Petch strengthening contribution σ_{HP} together with the average grain size d are shown in Table 4 and the stress-strain curves for the strain rate jump

tests in compression mode in air at room temperature, 750 and 900 °C are shown in Fig. 4.

This estimation shows that the Hall-Petch strengthening contribution is quite small and more or less negligible compared to the solid solution strengthening effect.

All three alloying elements lead to a significant increase in strength at room temperature as well as at 750 °C, with the Ti-33Al-5Zr alloy showing the highest strength, followed by Ti-33Al-5Ta and Ti-33Al-5Nb. This strengthening contribution is in the order of 100-200 MPa compared to the unalloyed binary alloy. The Ti-33Al, Ti-33Al-5Nb and Ti-33Al-5Ta alloys show a decrease in strength at larger strains, which could indicate a brittle failure as reported in literature for α_2-Ti_3Al alloys.[1,22,36]

The strength difference between the ternary Ti-33Al-5X alloys and the binary Ti-33Al alloy decreases when increasing the temperature to 750 and 900 °C. To further investigate the temperature and time dependent strength of

Table 4 Average grain size d and estimated Hall–Petch strengthening contribution σ_{HP} for the α_2-Ti_3Al alloys

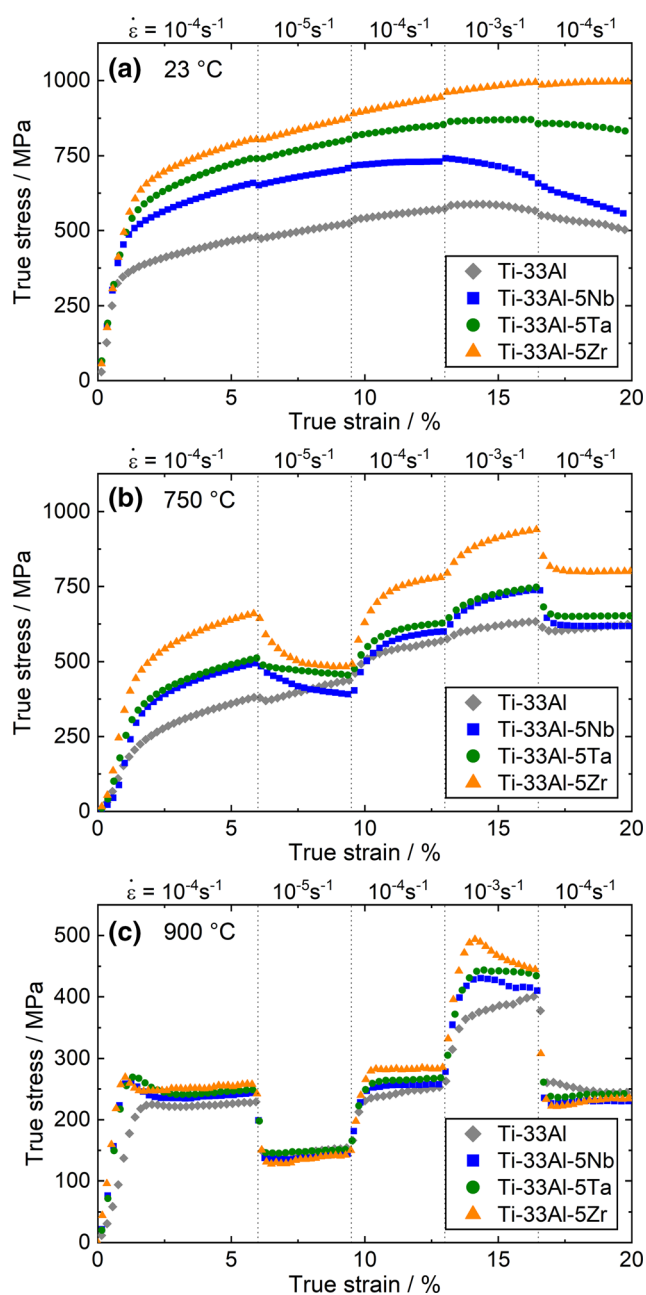| Alloy	Average grain size d, μm	Hall–Petch strengthening contribution σ_{HP}, MPa
Ti-33Al	491	18
Ti-33Al-5Nb	65	49
Ti-33Al-5Ta	45	59
Ti-33Al-5Zr	50	56

Fig. 4 Strain rate jump tests in compression mode in air at (a) 23 °C, (b) 750 °C and (c) 900 °C of the Ti-33Al-5X alloys and Ti33Al

the four investigated alloys, the 0.2% yield strength $\sigma_{p0.2}$ and strain rate sensitivity m at room temperature, 750 and 900 °C are shown in Fig. 5(a) and (b), respectively. It can be seen that the 0.2% yield strength for the ternary Ti-33Al-5X alloys decreases as the temperature increases,

while the strain rate sensitivity increases due to the increasing influence of thermally activated processes.

The results of the mechanical tests on the ternary Ti-33Al-5X alloys and the binary Ti-33Al alloy show similar trends as recently observed for single γ-phase alloys.[13] Similar to this recent study, the addition of Zr also leads to the greatest increase in strength, while the addition of Nb and Ta results in a smaller strength increase. Again, it seems that at lower temperatures and higher strain rates, the strength increase appears to be correlated with the solid solution hardening potential of the different alloying elements based on their Goldschmidt radii.[41] Apparently, the size difference between the solute and the surrounding matrix atoms provides the largest contribution to the strengthening. If the temperature increases and the strain rate decreases, the diffusivity increases, as indicated by the increasing strain rate sensitivity, and diffusion-controlled glide and climb process contribute more to the plastic deformation. Then, slower diffusing elements provide a higher strengthening contribution by a kinetic retardation effect on these glide and climb processes. This behavior has been already observed for various alloying elements in Ni.[48,49] This is also supported by the fact that Ti-33Al-5Ta, with the slower diffusing element Ta, shows the highest strength at the highest test temperature of 900 °C and the lowest applied strain rate of 10^{-5} s^{-1} while Ti-33Al-5Zr, with the faster diffusing element Zr, shows the lowest strength.

5 Summary and Conclusion

The influence of the alloying elements Nb, Ta and Zr on the diffusivity in α_2-Ti$_3$Al at temperatures between 1050 and 1150 °C was investigated using diffusion couples. To investigate the strengthening effects of these three alloying elements, strain rate jump tests in compression mode in air were carried out at room temperature, 750 and 900 °C. The following conclusion can be drawn from these investigations:

- Ta is the slowest diffusing element in single phase α_2-Ti-33Al, followed by Nb and Zr , which is similar to the diffusion behavior of these three elements in the γ-phase.

- The addition of 5 at.% Nb, Ta or Zr results in an increase in strength compared to a binary α_2-Ti-33Al alloy. At lower temperatures and faster strain rates, the
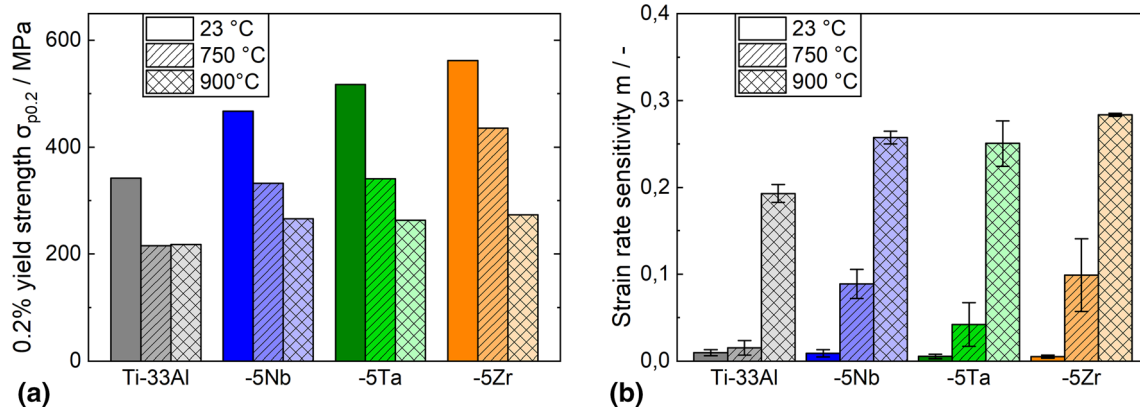
Fig. 5 (a) 0.2% yield strength $\sigma_{p0.2}$ and (b) strain rate sensitivity m of the Ti-33Al-5X alloys and Ti-33Al at 23, 750 and 900 °C

addition of Zr leads to the highest strength increase, followed by Ta and Nb, which is attributed to their atomic size mismatch, respectively. At higher temperatures and lower strain rates, the lower diffusivity of Ta becomes increasingly important, resulting in a higher strengthening potential than Nb and Zr.

References

1. F. Appel, J.D.H. Paul, and M. Oehring, *Gamma Titanium Aluminide Alloys: Science and Technology*. Wiley-VCH, Weinheim, 2011.
2. C. Leyens, M. Peters, Eds., *Titanium and Titanium Alloys: Fundamentals and Applications, Wiley-VCH* John Wiley (distributor), Weinheim, Chichester, 2003
3. Y.Y. Chen, F. Yang, F.T. Kong, and S.L. Xiao, Microstructure, Mechanical Properties, Hot Deformation and Oxidation Behavior of Ti–45Al–5.4V–3.6Nb–0.3Y alloy, *J. Alloys Compd.*, 2010, **498**, p 95–101. https://doi.org/10.1016/j.jallcom.2010.03.118
4. Y.-W. Kim, and S.-L. Kim, Advances in Gammalloy Materials–Processes–Application Technology: Successes, Dilemmas, and Future, *JOM*, 2018, **70**, p 553–560. https://doi.org/10.1007/s11837-018-2747-x
5. T. Noda, Application of Cast Gamma TiAl for Automobiles, *Intermetallics*, 1998, **6**, p 709–713. https://doi.org/10.1016/S0966-9795(98)00060-0
6. H. Clemens, and S. Mayer, Development Status, Applications and Perspectives of Advanced Intermetallic Titanium Aluminides, *Mater. Sci. Forum*, 2014, **783–786**, p 15–20. https://doi.org/10.4028/www.scientific.net/MSF.783-786.15
7. D.M. Dimiduk, Gamma Titanium Aluminide Alloys—An Assessment Within the Competition of Aerospace Structural Materials, *Mater. Sci. Eng. A*, 1999, **263**, p 281–288.
8. M. Es-Souni, A. Bartels, and R. Wagner, Creep Behaviour of Near γ-TiAl Base Alloys: Effects of Microstructure and Alloy Composition, *Mater. Sci. Eng. A*, 1995, **192–193**, p 698–706. https://doi.org/10.1016/0921-5093(94)03290-4
9. K. Maruyama, R. Yamamoto, H. Nakakuki, and N. Fujitsuna, Effects of Lamellar Spacing, Volume Fraction and Grain Size on Creep Strength of Fully Lamellar TiAl Alloys, *Mater. Sci. Eng. A*, 1997, **239–240**, p 419–428. https://doi.org/10.1016/S0921-5093(97)00612-6
10. H. Clemens, and S. Mayer, Advanced Intermetallic TiAl Alloys, *Mater. Sci. Forum*, 2016, **879**, p 113–118. https://doi.org/10.4028/www.scientific.net/MSF.879.113
11. Y.-W. Kim, Intermetallic Alloys Based on Gamma Titanium Aluminide, *JOM J. Miner. Met. Mater. Soc.*, 1989, **41**, p 24–30.
12. J. Bresler, S. Neumeier, M. Ziener, F. Pyczak, and M. Göken, The Influence of Niobium, Tantalum and Zirconium on the Microstructure and Creep Strength of Fully Lamellar γ/α₂ Titanium Aluminides, *Mater. Sci. Eng. A*, 2019, **744**, p 46–53. https://doi.org/10.1016/j.msea.2018.11.152
13. L. Haußmann, S. Neumeier, J. Bresler, S. Keim, F. Pyczak, and M. Göken, Influence of Nb Ta and Zr on the Interdiffusion Coefficients and Solid Solution Strengthening of γ-TiAl Single Phase Alloys, *Metals*, 2022, **12**, p 752. https://doi.org/10.3390/met12050752
14. C. Herzig, T. Przeorski, M. Friesel, F. Hisker, and S. Divinski, Tracer Solute Diffusion of Nb, Zr, Cr, Fe, and Ni in γ-TiAl: Effect of Preferential Site Occupation, *Intermetallics*, 2001, **9**, p 461–472. https://doi.org/10.1016/S0966-9795(01)00025-5
15. S. Divinski, F. Hisker, C. Klinkenberg, and C. Herzig, Niobium and Titanium Diffusion in the High Niobium-Containing Ti–

54Al–10Nb Alloy, *Intermetallics*, 2006, **14**, p 792–799. https://doi.org/10.1016/j.intermet.2005.12.007

16. T. Kawabata, H. Fukai, and O. Izumi, Effect of Ternary Additions on Mechanical Properties of TiAl, *Acta Mater.*, 1998, **46**, p 2185–2194. https://doi.org/10.1016/S1359-6454(97)00422-9

17. S. Neumeier, J. Bresler, C. Zenk, L. Haußmann, A. Stark, F. Pyczak, and M. Göken, Partitioning Behavior of Nb, Ta, and Zr in Fully Lamellar γ/α₂ Titanium Aluminides and Its Effect on the Lattice Misfit and Creep Behavior, *Adv. Eng. Mater.*, 2021. https://doi.org/10.1002/adem.202100156

18. J.B. Singh, G. Molénat, M. Sundararaman, S. Banerjee, G. Saada, P. Veyssière, and A. Couret, *In Situ* Straining Investigation of Slip Transfer Across α₂ Lamellae at Room Temperature in a Lamellar TiAl Alloy, *Philos. Mag. Lett.*, 2006, **86**, p 47–60. https://doi.org/10.1080/09500830500497066

19. J.B. Singh, G. Molénat, M. Sundararaman, S. Banerjee, G. Saada, P. Veyssière, and A. Couret, The Activation and the Spreading of Deformation in a Fully Lamellar Ti–47 at.% Al–1 at.% Cr–0.2 at.% Si Alloy, *Philos. Mag.*, 2006, **86**, p 2429–2450. https://doi.org/10.1080/14786430600606826

20. J.M.K. Wiezorek, X.D. Zhang, A. Godfrey, D. Hu, M.H. Loretto, and H.L. Fraser, Deformation Behavior of α2-Lamellae in Fully Lamellar Ti-48Al-2Mn-2Nb at Room Temperature, *Scr. Mater.*, 1998, **38**, p 811–817. https://doi.org/10.1016/S1359-6462(97)00538-1

21. Y. Mishin, and C. Herzig, Diffusion in the Ti–Al System, *Acta Mater.*, 2000, **48**, p 589–623. https://doi.org/10.1016/S1359-6454(99)00400-0

22. H.A. Lipsitt, D. Shechtman, and R.E. Schafrik, The Deformation and Fracture of Ti3Al at Elevated Temperatures, *Metall. Trans. A*, 1980, **11**, p 1369.

23. S.M.L. Sastry, and H.A. Lipsitt, Ordering Transformations and Mechanical Properties of Ti₃Al and Ti₃Al-Nb Alloys, *Metall. Trans. A*, 1977, **8**, p 1543–1552. https://doi.org/10.1007/BF02644857

24. R. Kainuma, Y. Fujita, H. Mitsui, I. Ohnuma, and K. Ishida, Phase Equilibria Among α (hcp), β (bcc) and γ (L10) Phases in Ti–Al Base Ternary Alloys, *Intermetallics*, 2000, **8**, p 855–867. https://doi.org/10.1016/S0966-9795(00)00015-7

25. S.S.A. Gerstl, Y.-W. Kim, and D.N. Seidman, Atomic Scale Chemistry of α₂/Interfaces in a Multi-component TiAl Alloy, *Interface Sci.*, 2004, **12**, p 303–310. https://doi.org/10.1023/B:INTS.0000028659.31526.2b

26. D.J. Larson, C.T. Liu, and M.K. Miller, The Alloying Effects of Tantalum on the Microstructure of an α2+γ Titanium Aluminide, *Mater. Sci. Eng. A*, 1999, **270**, p 1–8. https://doi.org/10.1016/S0921-5093(99)00233-6

27. Z.W. Huang, Thermal Stability of Ti–44Al–4Nb–4Zr–0.2Si–1B Alloy, *Intermetallics*, 2013, **42**, p 170–179. https://doi.org/10.1016/j.intermet.2013.06.007

28. V.M. Imayev, A.A. Ganeev, D.M. Trofimov, N.J. Parkhimovich, and R.M. Imayev, Effect of Nb, Zr and Zr + Hf on the Microstructure and Mechanical Properties of β-Solidifying γ-TiAl Alloys, *Mater. Sci. Eng. A*, 2021, **817**, p 141388. https://doi.org/10.1016/j.msea.2021.141388

29. A. Menand, B. Deconihout, E. Cadel, and D. Blavette, Atom-Probe Investigations of Fine-Scale Features in Intermetallics, *Micron*, 2001, **32**, p 721–729. https://doi.org/10.1016/S0968-4328(00)00079-2

30. J.M.K. Wiezorek, P.M. Deluca, M.J. Mills, and H.L. Fraser, Deformation Mechanisms in a Binary Ti-48 at.%Al Alloy with Lamellar Microstructure, *Philos. Mag. Lett.*, 1997, **75**, p 271–280. https://doi.org/10.1080/095008397179525

31. J.C. Schuster, and M. Palm, Reassessment of the Binary Aluminum-Titanium Phase Diagram, *J. Phase Equilib. Diffus.*, 2006, **27**, p 255–277. https://doi.org/10.1361/154770306X109809

32. K. Levenberg, A Method for the Solution of Certain Non-linear Problems in Least Squares, *Q. Appl. Math.*, 1944, **2**, p 164–168. https://doi.org/10.1090/qam/10666

33. F. Sauer, and V. Freise, Diffusion in binären Gemischen mit Volumenänderung, *Berichte Bunsenges. für Phys. Chem.*, 1962, **66**, p 353–362.

34. E.W. Hart, Theory of the Tensile Test, *Acta Metall.*, 1967, **15**, p 351–355. https://doi.org/10.1016/0001-6160(67)90211-8

35. A.K. Ghosh, On the Measurement of Strain-Rate Sensitivity for Deformation Mechanism in Conventional and Ultra-Fine Grain Alloys, *Mater. Sci. Eng. A*, 2007, **463**, p 36–40. https://doi.org/10.1016/j.msea.2006.08.122

36. S.A. Court, J.P.A. Löfvander, M.H. Loretto, and H.L. Fraser, The Influence of Temperature and Alloying Additions on the Mechanisms of Plastic Deformation of Ti₃Al, *Philos. Mag. A*, 1990, **61**, p 109–139. https://doi.org/10.1080/01418619008235561

37. J. Breuer, T. Wilger, M. Friesel, and C. Herzig, Interstitial and Substitutional Diffusion of Metallic Solutes in Ti₃Al, *Intermetallics*, 1999, **7**, p 381–388. https://doi.org/10.1016/S0966-9795(98)00115-0

38. Y.L. Hao, D.S. Xu, Y.Y. Cui, R. Yang, and D. Li, The Site Occupancies of Alloying Elements in TiAl and Ti₃Al Alloys, *Acta Mater.*, 1999, **47**, p 1129–1139.

39. C.L. Fu, R. Reed, A. Janotti, M. Kremar, On the Diffusion of Alloying Elements in the Nickel-Base Superalloys, in: Superalloys 2004 Tenth Int. Symp., TMS, 2004: pp. 867–876. https://doi.org/10.7449/2004/Superalloys_2004_867_876

40. S. Neumeier, H.U. Rehman, J. Neuner, C.H. Zenk, S. Michel, S. Schuwalow, J. Rogal, R. Drautz, and M. Göken, Diffusion of Solutes in fcc Cobalt Investigated by Diffusion Couples and First Principles Kinetic Monte Carlo, *Acta Mater.*, 2016, **106**, p 304–312. https://doi.org/10.1016/j.actamat.2016.01.028

41. V.M. Goldschmidt, Crystal Structure and Chemical Constitution, *Trans. Faraday Soc.*, 1929, **25**, p 253–283.

42. A. Janotti, M. Krčmar, C.L. Fu, and R.C. Reed, Solute Diffusion in Metals: Larger Atoms Can Move Faster, *Phys. Rev. Lett.*, 2004. https://doi.org/10.1103/PhysRevLett.92.085901

43. M.S.A. Karunaratne, P. Carter, and R.C. Reed, Interdiffusion in the Face-Centred Cubic Phase of the Ni–Re, Ni–Ta and Ni–W Systems Between 900 and 1300 °C, *Mater. Sci. Eng. A*, 2000, **281**, p 229–233. https://doi.org/10.1016/S0921-5093(99)00705-4

44. M.S.A. Karunaratne, and R.C. Reed, Interdiffusion of the Platinum-Group Metals in Nickel at Elevated Temperatures, *Acta Mater.*, 2003, **51**, p 2905–2919. https://doi.org/10.1016/S1359-6454(03)00105-8

45. M.S.A. Karunaratne, and R.C. Reed, Interdiffusion of Niobium and Molybdenum in Nickel Between 900–1300 °C, Defect Diffus, *Forum*, 2005, **237–240**, p 420–425. https://doi.org/10.4028/www.scientific.net/DDF.237-240.420

46. M.E. Kassner, and M.-T. Pérez-Prado, *Fundamentals of creep in metals and alloys*. Elsevier, Amsterdam, 2004.

47. G. Gottstein, Materialwissenschaft und Werkstofftechnik: physikalische Grundlagen, 4., neu bearb. Aufl, Springer Vieweg, Berlin, 2014.

48. H. ur Rehman, K. Durst, S. Neumeier, A. Sato, R. Reed, and M. Göken, On the Temperature Dependent Strengthening of Nickel by Transition Metal Solutes, *Acta Mater.*, 2017, **137**, p 54–63. https://doi.org/10.1016/j.actamat.2017.05.038

49. L. Haußmann, H. ur Rehman, D. Matschkal, M. Göken, and S. Neumeier, Solid Solution Strengthening of Mo Re, Ta and W in Ni during High-Temperature Creep, *Metals*, 2021, **11**, p 1909. https://doi.org/10.3390/met11121909